

DESIGN STUDY OF ALTERNATE INJECTOR AT PELLETRON ACCELERATOR FACILITY

N. Mehrotra[#], P.V. Bhagwat, A.K. Gupta, S. Krishnagopal, R.K. Choudhury, S. Kailas, R.G. Pillay^{\$}
 NPD, BARC, Mumbai – 400085 India; ^{\$}TIFR, Mumbai – 400005 India

Abstract

As part of Pelletron Accelerator Facility augmentation program, it is planned to have an alternate injector system to the Superconducting LINAC booster. The LINAC booster has been commissioned and is now operational to provide beams up to A~60 region with E~5 MeV/A. The development of an alternate injector will further enhance the utilization capability of booster LINAC by covering heavier mass range ($1/7 \leq q/m \leq 1/2$) with higher intensity up to Uranium. This injector system comprises of an Electron Cyclotron Resonance (ECR) ion source, Radio Frequency Quadrupole (RFQ) Linac and superconducting low-beta cavities. The design study from ion source to exit of RFQ is presented in this paper.

at $f/2$ (75 MHz) of the S-LINAC frequency, will accept beams with $\beta = 0.46\%$ and accelerate it up to $\beta = 3.5\%$. These beams would then go through two sets of superconducting cavities with $\beta = 5.0\%$ and $\beta = 7.0\%$, respectively. This acceleration is expected to bring all ion beams from carbon to uranium, to the velocity range $\beta = 8-10\%$ which is suitable for S-LINAC acceptance. After further acceleration through S-LINAC, light ions of about 12 MeV/u and uranium ions of about 7 MeV/u would be available on target.

The final energies available from this alternate injector system would vastly enhance the capability of S-LINAC as a research tool for nuclear physics. The low-beta cavities design will be discussed in a subsequent paper.

INTRODUCTION

The 14 UD Pelletron Accelerator Facility (PAF), set up as a collaborative project between Bhabha Atomic Research Centre and Tata Institute of Fundamental Research, has been a major facility for both basic and applied research in India. The accelerator utilization for basic sciences constitutes about 70% of the total beam time.

Prior to injection into Superconducting LINAC (S-LINAC), the ion beam needs to be accelerated to 12-14 MV/q. The ion beam extracted from ECR ion source and pre-accelerated to required energy (10 keV/u), will be transported by Low Energy Beam Transport (LEBT) line (consisting of focusing, bending, and diagnostic elements) to the entrance of the heavy ion RFQ (see Fig. 1).

ECR ION SOURCE

The alternate injector and S-LINAC combination aims to accelerate U^{34+} ($q/m \sim 1/7$) ions with 100 pna yield on the target. To realize this, 18 GHz superconducting ECR ion source is the appropriate choice, which requires only 20 kW of power and 200 l/hr of cooling. An advanced version of this state-of-the-art ECR ion source, to be procured from M/s Pantechnik, France, is currently under development at their site. This source will be equipped with a mass selection feature on a high voltage platform of 300 kV, making it readily available as a stand-alone facility, till the development of the downstream elements is completed. This facility will be capable of generating highly charged positive ion beams with $0.3 \cdot q$ MeV for a wide range of elements across the periodic table. However, for injecting in to RFQ it will operate at 70 kV for U^{34+} producing about $3 \mu A$ of U^{34+} . Beside high yields of Group I, II elements like Na, K, Ca, Ba, the ECR ion source also produces beams of group VIII elements i.e. Ne, Ar, Kr etc. which cannot be produced in the present SNICS negative ion source of pelletron accelerator.

PREBUNCHER

Although the internal shaper and buncher of RFQ have almost 100% capture and bunching efficiencies, it is at the cost of increased length and power consumption. Hence, it was decided to have a 75 MHz prebuncher with three of its harmonics 40 cm upstream RFQ. The phase capture for the third harmonic buncher is 75%. The buncher to RFQ distance (s) was optimised using an analytical formula (see Eq. 1) derived by Fourier series analysis of saw-tooth waveform

$$s = \beta \lambda \frac{\phi}{2F(\phi)} \frac{E(\text{keV/u})}{(Z/\zeta)U(\text{kV})}, F(\phi) = \sum_{n=1}^{n=3} (-1)^{n+1} \frac{\sin(n\phi)}{n} \quad (1)$$

where $\beta = v/c$, v being the velocity of incoming ions, ϕ is the phase at which $F(\phi)$ is maximum, Z/ζ is the ratio of

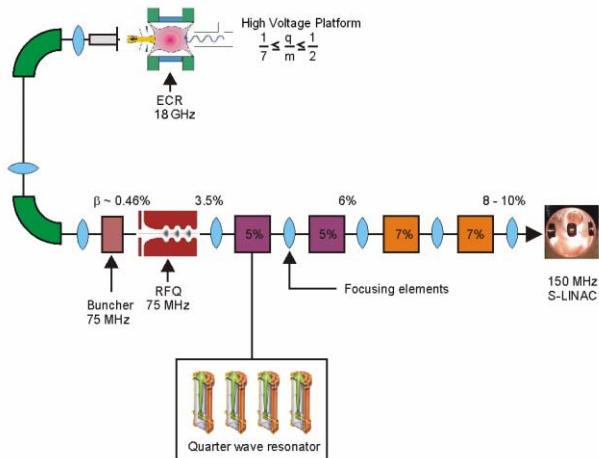


Figure 1: Alternate Injector Layout.

To reduce the RFQ length, a buncher operating at same frequency as RFQ was also finalized. The RFQ operating

[#]mehrotra@tifr.res.in

atomic number to mass number for the respective ions. All heavy ions with different Z/ζ can be bunched in the same drift length by keeping $ZU(\text{kV})/\zeta$ constant, as all ions will have same β (see Fig. 2). The maximum bunching voltage was determined from maximum energy spread accepted by the first cell of RFQ (see Eq. 2).

$$\Delta W/u = [(qU_0/m) \beta_s^2 c^2 A_{10} (\phi_s \cos \phi_s - \sin \phi_s)]^{1/2} \quad (2)$$

For our case, $\phi_s = -90^\circ$, $m = 1.001$, $\Delta W = 0.285 \text{ keV/u}$. This corresponds to bunching voltage of 2.1 kV. The prebuncher will focus the beam at the exit of RMS to minimize longitudinal defocusing of the beam, howsoever small, in the RMS.

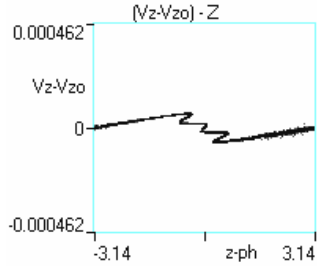


Figure 2: Bunched beam at RFQ entry.

RFQ LINAC

Among the ultra low velocity accelerating structures for heavy ions, RFQ holds merit in terms of beam quality and efficient acceleration. The choice of operating frequency of 75 MHz was driven by S-LINAC frequency and power dissipation in the RFQ. The pre-acceleration voltage (V) was then decided by the capability to machine the first RFQ cell i.e. the cutting tool should be able to cut cells of length $\beta\lambda$ and depth $m^*(a-1)$. Hence, $V = 10*m/q$ was selected so that the first period has a length of 1.8cm.

Radial Matching Section (RMS)

The RMS consisting of 8 cells, of which the first 2 cells form the flange and gap to vane, matches the spatially focussed beam to the transient focussing and acceptance of the RFQ. It was optimized using our analysis [1] as outlined below. Starting with the potential function

$$U(r, \theta, z) = \frac{U_0}{2} \sum_{m=1}^n \sum_{n=1}^m A_{mn} I_n(mkr) \cos(n\theta) \sin(mkz)$$

where, $m=2s+1$, $n=2(2p+1)$, $s, p=0,1,2\dots$ and taking first two terms for quadrupolar symmetry, the analytical results for vane profile in RMS is given by

$$(a/r_0)^2 = 2/[Sinkz(3 - Sin^2 kz)] \quad (3)$$

The vanes cannot be extended to the cavity end walls. Hence, this profile becomes inadequate. It is then scaled up according to

$$a_{new}/r_0 = s(a/r_0 - 1) + 1 \quad (4)$$

s being the scaling parameter. The choice of scaling factor was then optimized (see Fig. 3) using LIDOS.RFQ.DESIGNER [2]. Eqs. 3 and 4 were then used to generate the longitudinal vane profile in RMS (see Fig. 4). With this vane profile, mismatching of 1.04 and 95% overlap of particle ellipses with the acceptance ellipse was achieved. This optimisation leads

to low amplitude envelope oscillations caused by the mismatched input beam.

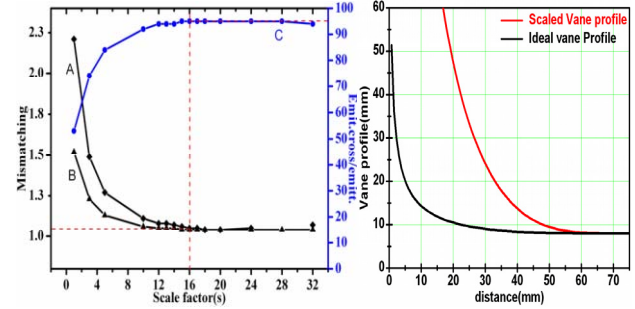


Figure 3: Scale factor Opt..

Figure 4: Vane profile.

Cell Parameters

This heavy ion RFQ was designed with constant mean aperture radius (r_0) in order to keep the intervane capacitance per unit length constant. The smooth variation approach was utilized for optimizing modulation and phase in the design (see Fig. 5).

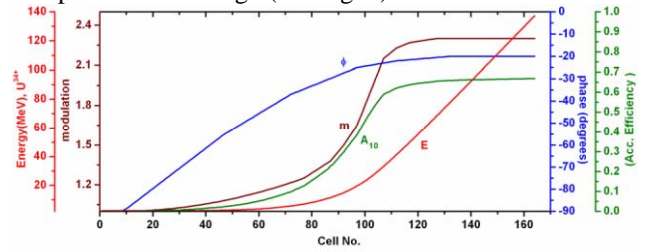


Figure 5: Cell parameters along RFQ.

A short bunching section was introduced to capture some part of 25% unbunched beam. This explains the slow variation of phase along the RFQ. The defocusing factor was increased faster to take advantage of the already bunched beam (see Fig. 6). Due to this, the longitudinal and transverse phase advances cross over (see Fig. 7). The salient feature of this design is the final phase of -20° .

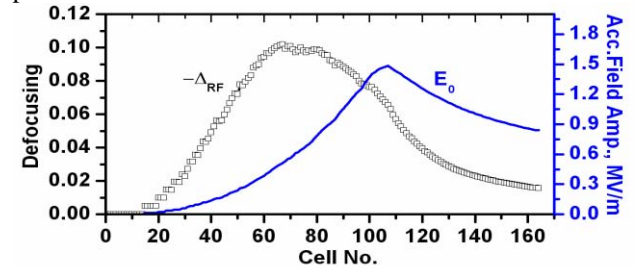


Figure 6: Defocusing & Acc. Field Amp. along RFQ.

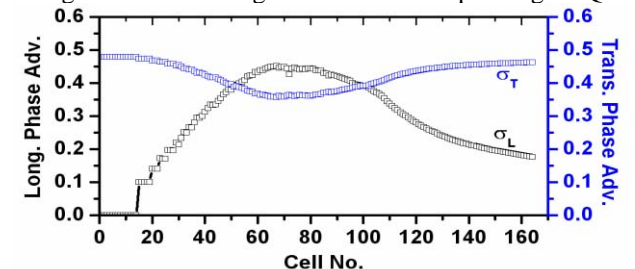


Figure 7: Phase Advance along RFQ.

Vane Design

Extensive simulations were done to optimize vane related parameters. Near the beam axis, the vane geometry is approximated by circular arcs instead of hyperbolae in the transverse plane. Based on simulations (see Fig. 8), the following parameters were zeroed on.

Table 1: Vane Parameters

| | |
|------------------------------|-------|
| ρ/r_0 | 0.875 |
| Incl. Angle of Vane-Tip, deg | 21.0 |
| Semi-Width of Vane Tip, mm | 12.5 |

A ρ/r_0 value of 0.875 was chosen to lower the peak surface electric fields while maintaining good transmission. Inclination angle of 21 degrees was chosen to bring the vane profile close to the ideal two-term vane profile (see Fig. 9). The choice of semi-width of vane tip has more to do with the droop of vanes and cooling requirement than controlling the intervane capacitance.

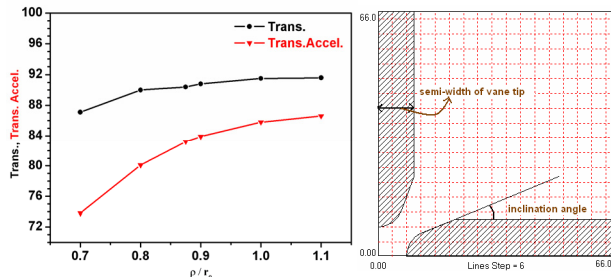


Figure 8: ρ/r_0 Optimization. Figure 9: Vane Shape.

PIC Simulation

Particle In Cell (PIC) simulations were performed using LIDOS for gaussian distribution with 50,000 particles and real vane shape. A simulated transmission of **92.5%** and **87%** of Trans. Accel. was obtained. Trans. Accel. is a measure of transmission of longitudinally accelerated particles. A phase width of $\pm 9^\circ$ and momentum spread of $\pm 0.35\%$ was obtained at the exit of RFQ (see Fig. 10). The table below summarises the final RFQ parameters.

Table 2: RFQ Specifications

| | |
|-----------------------------------------|----------------------------|
| q/m | 1/7, U 34+ |
| Ein / Eout, keV/u | 10 / 575 |
| Frequency, MHz | 75 |
| Kilpatrick Factor | 1.4 |
| Focussing Parameter (B) | 4.26 |
| Intervane Voltage, kV | 16*m/q |
| Mean Aperture Radius (r_0) | 8.0 mm |
| Minimum Aperture (a), mm | 8.0-4.51 |
| Current (I), mA | 0.1 |
| ϵ (input, norm.) π mm mrad | 1.0 |
| Modulation (m) | 1.0 - 2.3 |
| Synchronous Phase (ϕ_s) | -90° to -20° |
| Number of cells (n) | 167 |
| Length, m | 4.62 |
| RMS Long. Emitt., keV/u*ns | 0.3 |

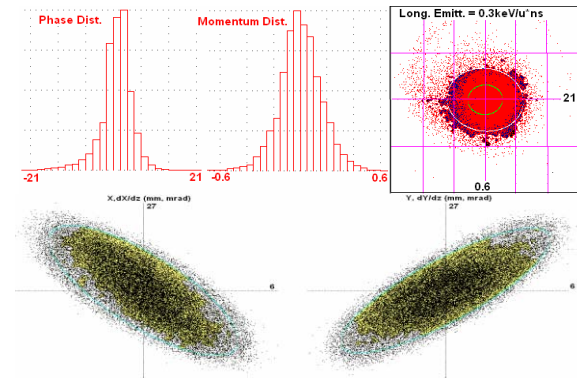


Figure 10: Output Characteristics of beam at RFQ exit.

Sensitivity (or Error) Study

The effect of errors arising due to improper vane machining and misalignment, on the performance of RFQ, was studied using the statistics module of LIDOS. Perturbations in vane voltage (dU/U), modulation (dm) and average cell radius (dR) were simulated separately and simultaneously as well. At the beginning of each cell, the code adds uniformly distributed random deviations on the specified cell parameter over \pm tolerance level. Cell radius (dR) varies as cubic spline while voltage and modulation vary as linear spline along the accelerator length. The cell-to-cell random deviations are statistically independent. Based on simulations with 10,000 particles and 9 statistical realizations, $dU/U = 0.04$, $dm = 0.05$ and $dR = 0.1\text{mm}$ was acceptable for Trans. Accel. greater than 84% (see Fig. 11). When these errors were simulated simultaneously, Trans. Accel. dropped to 72.6%.

Alignment errors were also simulated with a linear symmetric taper separately. From positive taper (away from axis) of $200\mu\text{m}$ to negative taper of $200\mu\text{m}$ (towards axis) along the RFQ length, Trans. Accel. was within 1% of zero taper value. A negative taper was preferred, even at the cost of increasing surface field, to keep Long./Trans. frequency in check and to maintain adequate transverse focusing.

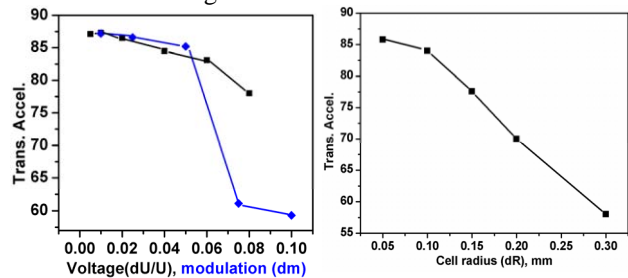


Figure 11: Tolerance Study.

REFERENCES

- [1] N. Mehrotra, P. V. Bhagwat and M. B. Kurup, "Optimisation of the Radial Matching Section for the Prototype RFQ", NIM A 545 (2005) 57-62.
- [2] LIDOS.RFQ.DESIGNER™ Version 1.3, <http://www.ghga.com/accelsoft/>.